Dynamic Behavior of a 2 Variable Speed Pump-Turbine Power Plant

[(1)]Y. Pannatier, [(2)] C. Nicolet, [(1)]B. Kawkabani[(*)], [(1)]J.-J. Simond[(*)], [(1)]Ph. Allenbach
[(*)]Member IEEE
[(1)]Ecole Polytechnique Fédérale de Lausanne, EPFL-STI-IEL-LME
[(1)]ELG 132, Station 11, CH-1015 Lausanne, Switzerland, Phone: (+41) 21 693 46 90, e-mail: yves.pannatier@epfl.ch
[(2)] Power Vision Engineering Sàrl, CH-1024 Ecublens, Switzerland

***Abstract*- This paper presents the modeling, simulation and analysis of the dynamic behavior of a fictitious 2x320 MW variable speed pump-turbine power plant including hydraulic system, electrical equipments, rotating inertias and control systems using the software SIMSEN. First, the modeling of hydraulic and electrical components of the power plant is presented. Then the pseudo continuous approximation is introduced. It consists in a simplification of the electrical part of the power plant. Thanks to this simplification, simulation time can be reduced drastically (~ factor 60). The complete and simplified models are compared by simulation and the validity of the pseudo continuous approximation is discussed. Finally two control strategies in generating mode are implemented and compared by simulation.**

I. Introduction

Variable speed pump-turbine units have become nowadays an interesting way to increase stability of electrical power networks due to their high level of operating flexibility. Indeed, variable speed pump-turbine units offer several advantages for both pumping and generating modes such as: (i) possibility of active power control in pumping mode, (ii) efficiency increase and wide range of operation in generating mode especially under partial load, (iii) network stability improvement by reactive power control and (iv) network stability improvement by instantaneous active power injection in the grid (flywheel effect). For operating stability purposes, the increase of dynamic performance is of major concerns and its optimization requires reliable simulation models.

II. Modeling of the Power Plant

The complete model of the power plant comprising the hydraulic and electrical systems is presented in Fig.1.

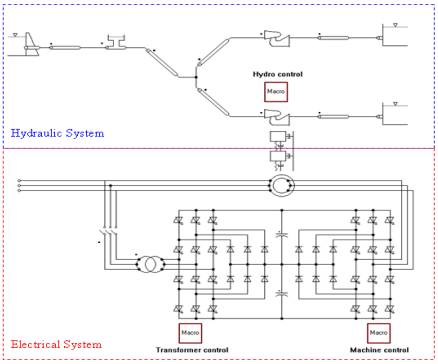

Fig.1. Complete model of the power plant

A. Modeling of the hydraulic system

The layout of the hydraulic system is presented in Fig.2 and is made of an upstream reservoir, a 600 meters long gallery, a 18 meters diameter surge tank, a 900 meters long penstock connected to Francis pump-turbines 320 MW. The main parameters of the pump-turbines are presented in Table I while the pump-turbine characteristics are presented in Fig.3. It can be noticed that these ones feature the so-called S-shape curve in the 1st and 4th quadrants.

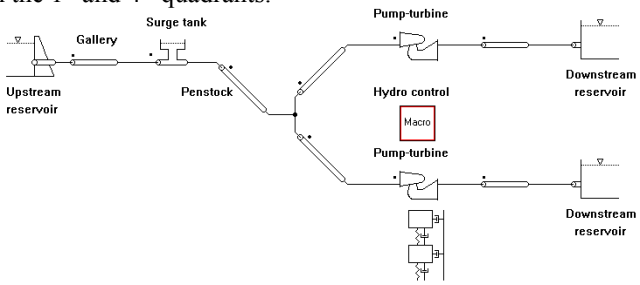

Fig.2. Hydraulic system of the power plant

TABLE I
Rated Values Of The Pump-Turbine

H_n [m]	Q_n [m³/s]	P_n [MW]	N_n [tr/min]	ν [-]	J [Kgm²]
552	64	320	450	0.2	1.8605e6

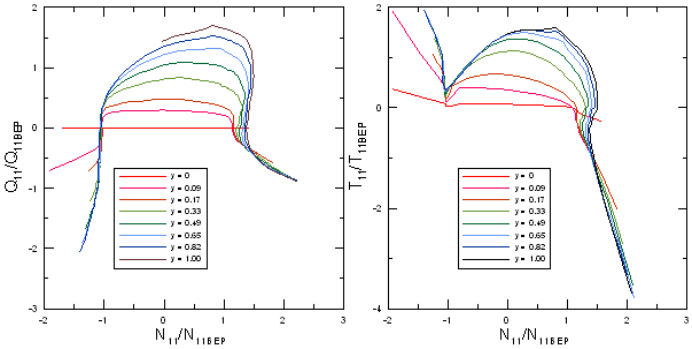

Fig.3. Pump-turbine characteristics

N_{11}, Q_{11} and T_{11} are dimensional factors defined from the speed N, the discharge Q, the torque T, the head H and the reference diameter of the pump-turbine D_{ref} as follows:

$$N_{11} = \frac{N \cdot D_{ref}}{\sqrt{H}} \quad Q_{11} = \frac{Q}{\sqrt{H} \cdot D_{ref}^{\,2}} \quad T_{11} = \frac{T}{H \cdot D_{ref}^{\,3}} \qquad (1)$$

Modeling of the different hydraulic components is based on an electrical analogy. For example, the procedure necessary to model a pipe is developed in this section.

By assuming uniform pressure and velocity distributions in the cross section and neglecting the convective terms, the one-dimensional momentum and continuity balance equations for an elementary pipe filled with water of length *dx*, cross section *A* and wave speed *a*, see Fig.4, yields to the following set of hyperbolic partial differential equations [6]:

$$\begin{cases} \dfrac{\partial h}{\partial t} + \dfrac{a^2}{gA} \cdot \dfrac{\partial Q}{\partial x} = 0 \\ \dfrac{\partial h}{\partial x} + \dfrac{1}{gA} \cdot \dfrac{\partial Q}{\partial t} + \dfrac{\lambda |Q|}{2gDA^2} \cdot Q = 0 \end{cases} \qquad (2)$$

The system (2) is solved using the Finite Difference Method with a 1st order centered scheme discretization in space and a scheme of Lax for the discharge variable. This approach leads to a system of ordinary differential equations that can be represented as a T-shaped equivalent scheme [1], [3], [5] as presented in Fig.5. The RLC parameters of this equivalent scheme are given by:

$$R = \frac{\lambda \cdot |\overline{Q}| \cdot dx}{2 \cdot g \cdot D \cdot A^2} \quad L = \frac{dx}{g \cdot A} \quad C = \frac{g \cdot A \cdot dx}{a^2} \qquad (3)$$

where λ is the local loss coefficient. The hydraulic resistance R, the hydraulic inductance L, and the hydraulic capacitance C correspond respectively to energy losses, inertia and storage effects.

The model of a pipe of length *L* is made of a series of n_b elements based on the equivalent scheme of Fig.5. The system of equations relative to this model is set-up using Kirchoff laws.

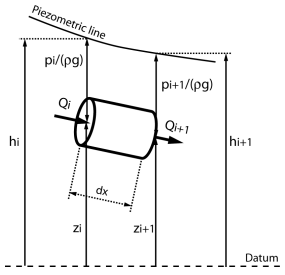

Fig.4. Elementary hydraulic pipe of length dx.

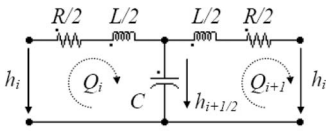

Fig.5. Equivalent circuit of an elementary pipe of length dx.

As presented in Table II, the modeling approach based on equivalent schemes of hydraulic components is extended to all the standard hydraulic components such as the surge tank and the Francis pump-turbine, see [2].

TABLE II
MODELING OF HYDRAULIC COMPONENTS WITH RELATED EQUIVALENT SCHEMES

Component	Hydraulic scheme	Electrical equivalent scheme	Parameters
Generalized pipe		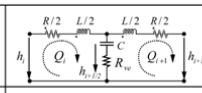	$R=\frac{d\alpha\lambda\|Q\|}{2gDA^2}$ $R_w=\frac{\mu}{\rho gAdx}$ $L=\frac{dx}{gA}$ $C=\frac{dxgA}{a^2}$
Surge tank	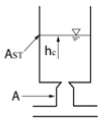	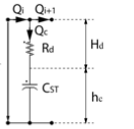	$R_d=\frac{K_d(Q)\|Q\|}{2gA^2}$ $C_{ST}=A_{ST}(h_c)$
Francis pump-turbine	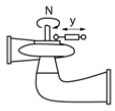	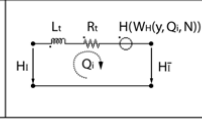	$H=H(W_H(y,Q,N))$ $T=T(W_B(y,Q,N))$ $R_t=R_t(W_H(y,Q,N))$ $L_t=\frac{l_{ew}}{gA}$

V_g : volume of gas [m³] W_H : turbine head characteristic [-] l_{ew} : turbine equivalent length [m]
h_g : pressure of gas [m] W_B : turbine torque characteristic [-] μ : viscosity of the fluid or material [Pa·s]

These models are finally implemented in the EPFL software SIMSEN, developed for the simulation of the dynamic behavior of hydroelectric power plants, [2], [4]. The time domain integration of the full system is achieved in SIMSEN by a Runge-Kutta 4th order procedure.

B. Modeling of the electrical system

The complete model of the electrical system comprises a doubly - fed induction generator, whose main parameters are presented in Table III, with VSI (Voltage Source Inverter) cascade in the rotor side. This electrical system can be divided into two sections, a transformer section and a machine one, as identified in Fig.6.

TABLE III
RATED VALUES OF THE GENERATOR

N_n [t/min]	S_n [MVA]	U_n [kV]	f_n [Hz]	2p [-]	s_{max} [%]
450	380	18	60	16	7

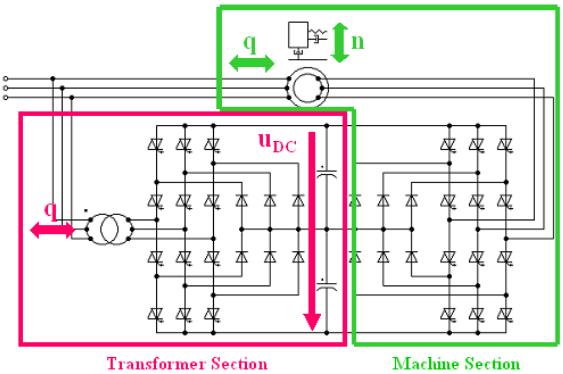

Fig.6. Electrical system of the power plant

The transformer section operates as a Static Var Compensator (SVC), its main role being to exchange reactive power with the grid. The reactive power and the capacitors voltage can be controlled by acting on the transformer primary side currents through the left-side converter. The control structure is shown in Fig.7, see [8].

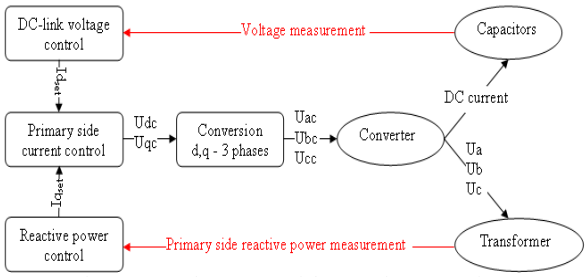

Fig.7. Control structure of the transformer section

The main role of the machine section is to control the speed of the machine. The speed and the stator reactive power of the machine can be controlled by acting on the rotor currents through the right-side converter. The control structure is shown in Fig.8, see [8].

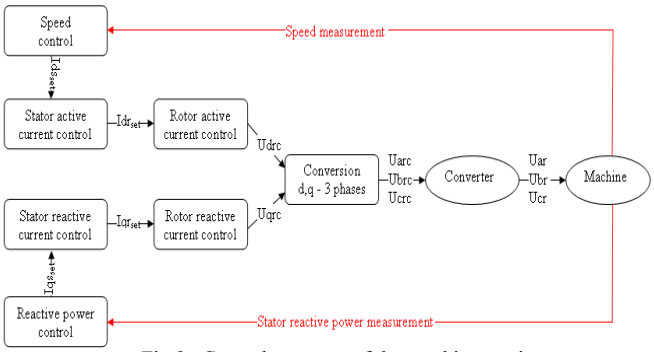

Fig.8. Control structure of the machine section

III. Pseudo Continuous Approximation

Voltage Source Inverters require a very small integration step, which results in expensive time consuming simulations. Simulation time can be considerably reduced by using a pseudo continuous approximation of the cascade, which consists in replacing the voltage source inverter on the rotor side by three controlled voltage sources and suppressing the inverter on the transformer side. As there is no more physical link between the rotor and the grid, see Fig.9, the rotor power transit with the grid has to be taken into account through a calculation block included in the machine control.

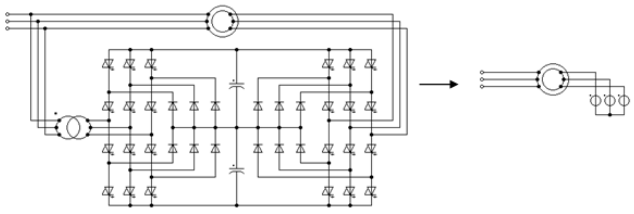

Fig.9. Complete and pseudo continuous models

IV. Control Strategies

In generating mode, two control strategies are investigated. The first strategy is illustrated in Fig.10 and considers turbine power governor and generator speed controller, see [7].

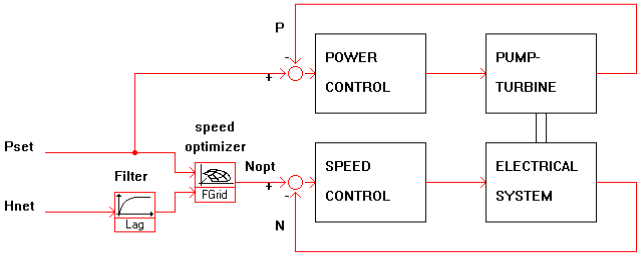

Fig.10. First strategy in generating mode

The speed control structure is shown in Fig.8. The power control is detailed in Fig.11 and consists of a PI type regulator whose output acts on the guide vane opening through a servomotor. The maximum displacement speed of the servomotor is fixed by a rate limiter.

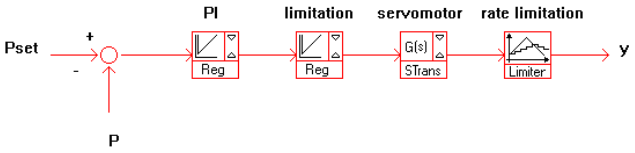

Fig.11. First strategy: power control structure

The second strategy is presented in Fig.12 and based on turbine speed governor and generator power controller, see [7].

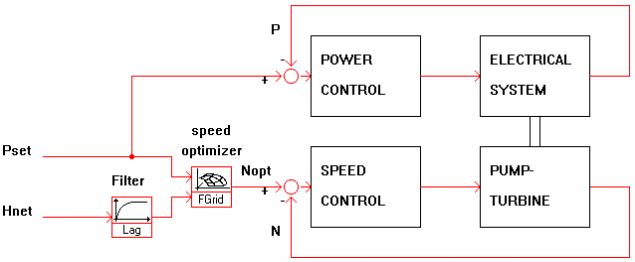

Fig.12. Second strategy in generating mode

The power control structure can be deduced from the structure detailed in Fig.8 by simply replacing the speed control block by a power control block. The speed control is shown in Fig.13 and consists of a PID type regulator acting on the guide vane opening as explained before.

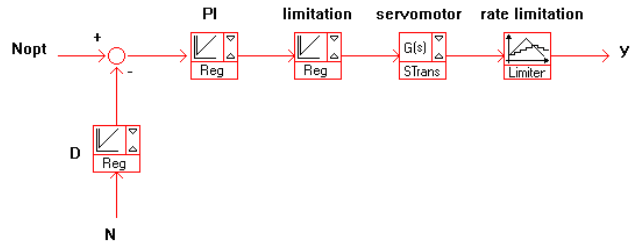

Fig.13. Second strategy: speed control structure

The power set point is imposed by the grid conditions and the speed set point is calculated by a speed optimizer in order to maximize the turbine efficiency. This speed optimizer is a surface representing the optimal speed as a function of the power and the head. This surface is shown in Fig.14 and is calculated from the pump-turbine characteristics defined in Fig.3. The optimum rotational speed is calculated from the dimensionless turbine characteristic, from which efficiency hill-charts are deduced as function of head and mechanical power for different rotational speeds N_i via interpolation process. For each combination of head and power in the operating range of the turbine, the rotational speed presenting the highest efficiency is selected. This approach provides the speed look-up table of Fig.14. It might be noticed that, as expected, the optimum rotational speed is the lowest for low power under low head, and is the highest for high power under high head.

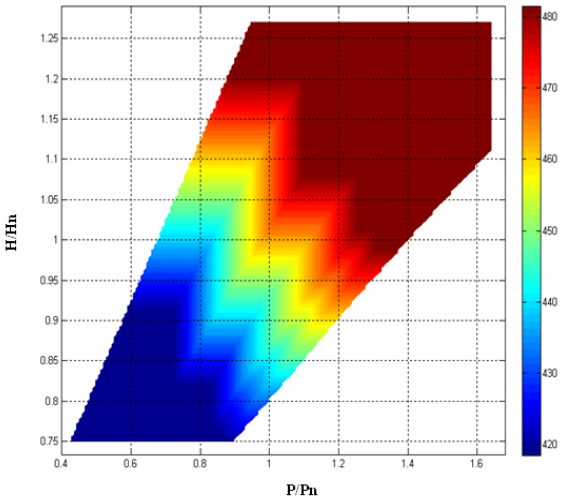

Fig.14. Speed look-up table N=N(H/Hn, P/Pn)

V. SIMULATION RESULTS

The simulation results are presented for both strategies 1 and 2 in generating mode, for a decrease of the active power set point. As shown in Fig. 15, the new speed set point is calculated by the speed optimizer depending on the new power set point and the head.

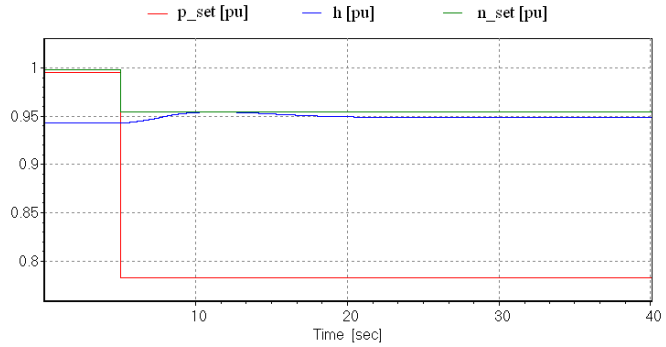

Fig.15. Power set point (red), filtered head (blue) and speed set point (green) in (pu)

A. *Strategy 1*

Concerning the first strategy, the new speed set point is reached very fast in about 4 seconds, because the speed is controlled by the electrical system (Fig.16).

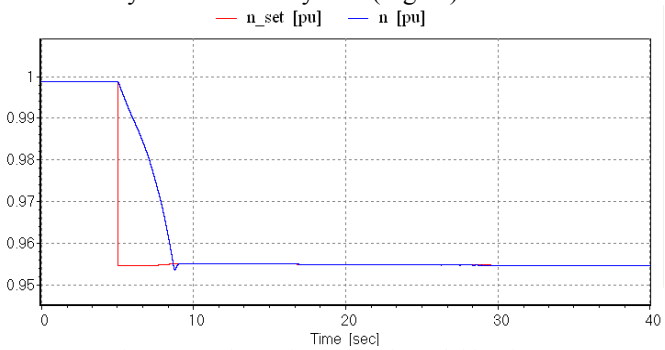

Fig.16. Speed set point (red) and speed (blue) in (pu)

This speed diminution leads to a power injection in the grid resulting from the transfer of kinetic energy from the rotating inertia to the grid. This phenomenon is called flywheel effect (Fig.17). Then the power is slowly regulated by the pump-turbine as illustrated in Fig. 17. Simulated results obtained by the first strategy show that the transient behavior (particularly the active power represented in Figure 17) following the set point variation of the active power is not acceptable and thus this strategy cannot be applied. The use of a rate limitation of the set point of the speed controller is necessary in order to avoid the undesirable transients of the active power. Figure 18 represents in per unit the head h, the discharge q, the torque t, the speed n and the turbine guide vane opening y.

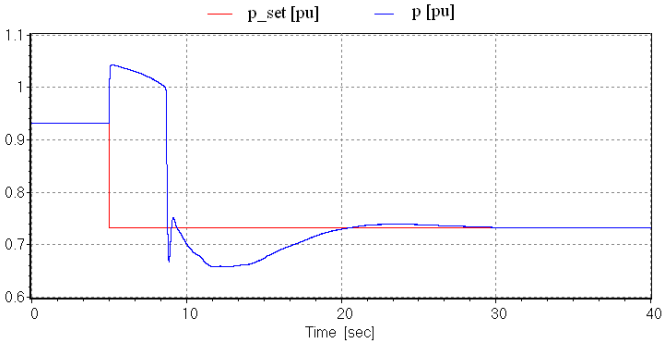

Fig.17. Power set point (red) and power (blue) in (pu)

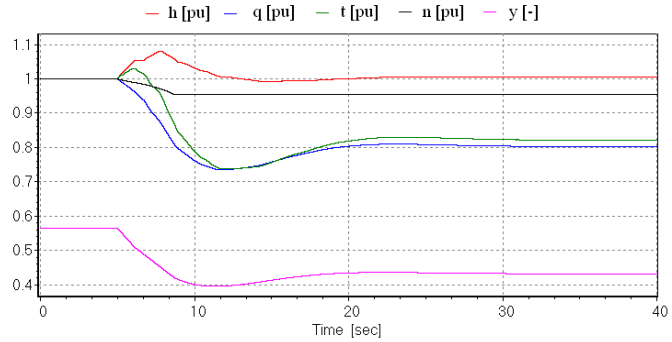

Fig.18. Transient behaviour of the pump-turbine in (pu)

In order to validate the pseudo-continuous approximation, these results can be compared with those obtained when considering the complete model of the rotor cascade (Fig.19).

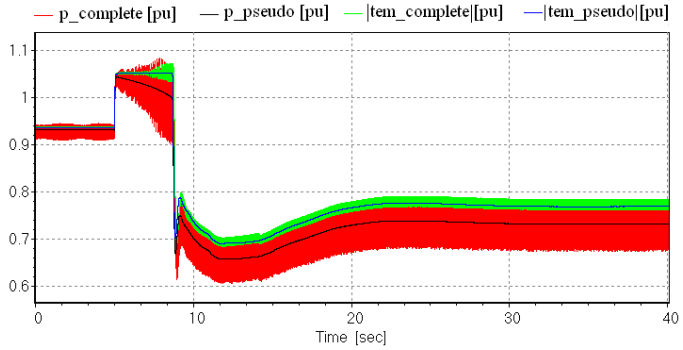

Fig.19. Comparison of the power and the electromagnetic torque (absolute value) obtained with the pseudo-continuous respectively the complete models

One can notice that there is a very good agreement between the results obtained by the two models. Using such pseudo-continuous model leads to a computation time reduction of factor 60 compared to the computation time obtained with the complete model. On the other hand, the complete model permits a precise analysis of the harmonics due to the converters. Indeed, a VSI converter introduces harmonics of ranges $6k \pm 1$ in the rotor currents, whose fundamental frequency is $s \cdot f_n = s \cdot 60$ [Hz] (Fig.20). These current harmonics lead to harmonics of ranges $6k$ in the electromagnetic torque (Fig.21).

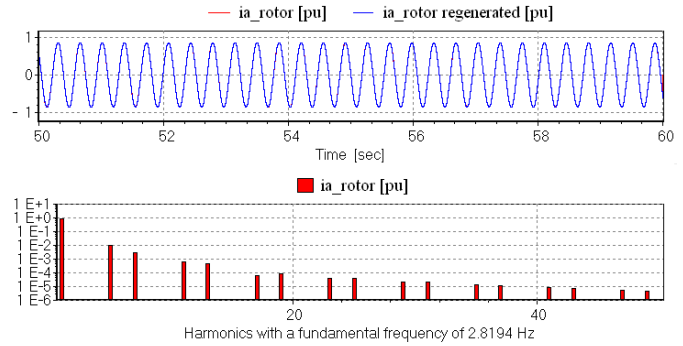

Fig.20. Complete model: frequency analysis of the rotor current in phase a

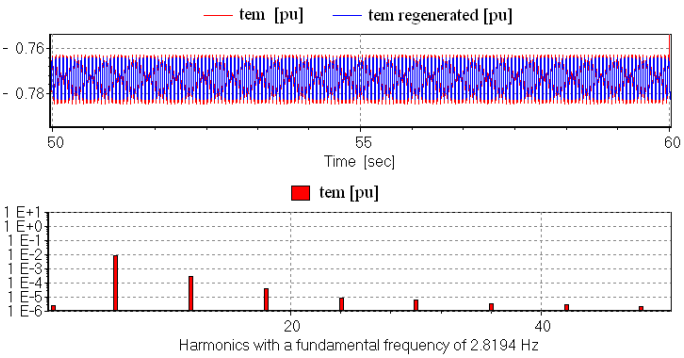

Fig.21. Complete model: frequency analysis of the electromagnetic torque

B. *Strategy 2*

Concerning the second strategy, the new power set point is reached very fast in less than 0.3 second because the power is controlled by the electrical system as presented in Figure 22.

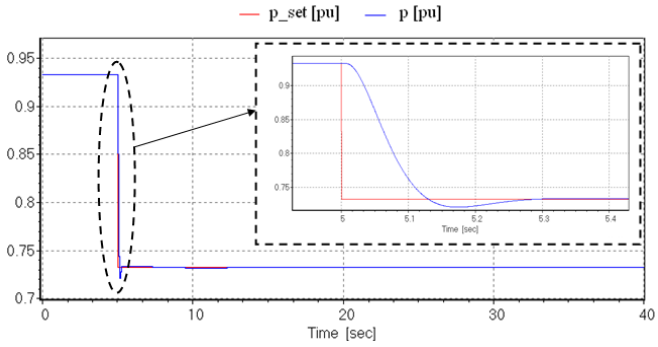

Fig.22. Power set point (red) and power (blue) in (pu)

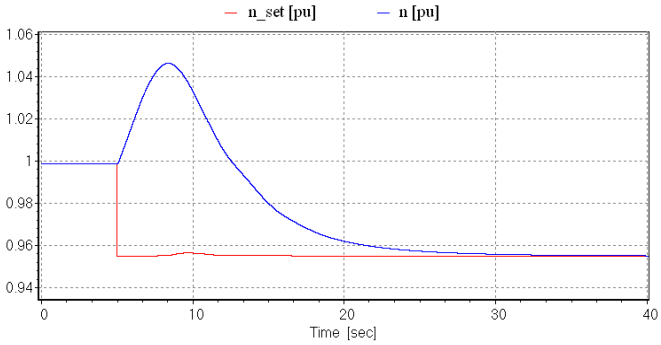

Fig.23. Speed set point (red) and speed (blue) in (pu)

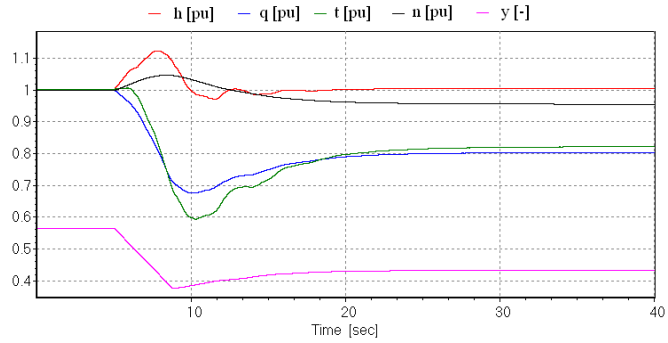

Fig.24. Transient behaviour of the pump-turbine in (pu)

This power diminution leads to an acceleration of the machine resulting from the accumulation of kinetic energy in the rotating inertia. Then the speed is slowly regulated by the pump-turbine as shown in Figures 23 and 24.

A comparison between these results and those obtained with the complete model of the rotor cascade confirms the validity of the pseudo-continuous approximation (Fig.25 and 26).

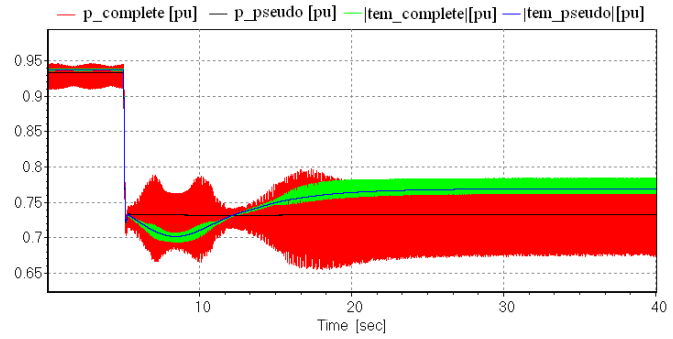

Fig.25. Comparison of the power and the electromagnetic torque (absolute value) obtained with the pseudo-continuous respectively the complete models

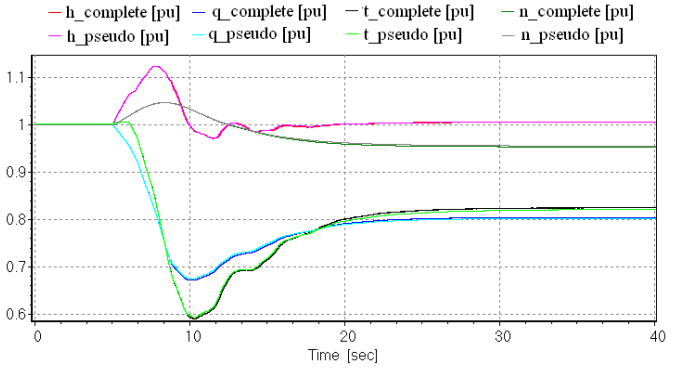

Fig.26. Comparison of the transient behavior of the pump-turbine obtained with the pseudo-continuous and the complete models

C. *Comparison of the two strategies in generating mode*

It's finally interesting to compare the dynamic behaviour resulting from strategies 1 and 2 in terms of both active and rotational speed variations as presented respectively in Fig.27 and Fig. 28.

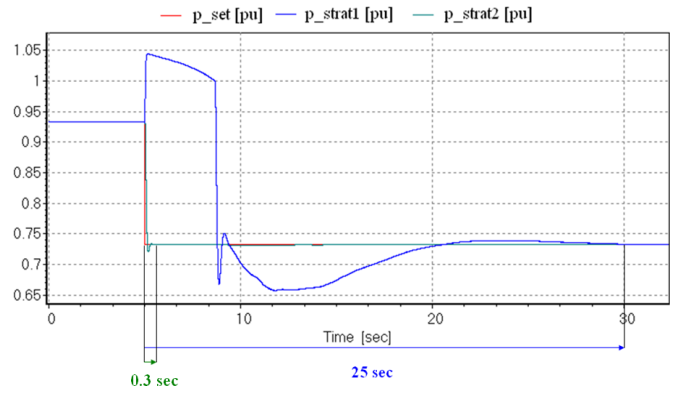

Fig.27. Power set point (red), power with strategy 1 (blue) and power with strategy 2 (green) in (pu)

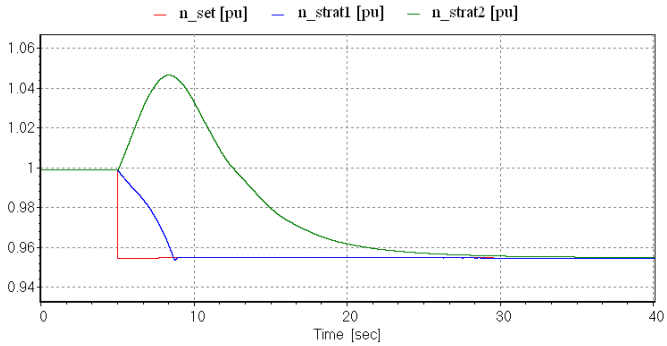

Fig.28. Speed set point (red), speed with strategy 1 (blue) and speed with strategy 2 (green) in (pu)

One can notice that the second strategy is capable of power set point changes about 84 times faster than using the first strategy, and therefore this strategy will be preferred.

VI. Conclusion

The behavior of a fictitious 2x320 MW variable speed pump-turbine power plant including hydraulic, electrical and control systems has been simulated in steady-state and transient conditions. Two control strategies in generating mode have been compared and the dynamic performances pointed out. A pseudo-continuous approximation related to the rotor cascade has been presented and validated by comparison with the complete model. A very important gain in the computation time (factor of about 60) is obtained by using this approach.

Acknowledgment

The authors would like to gratefully thank the partners of this project ALSTOM Power Hydro Dr A. Schwery in Birr, Switzerland and Mr J.-L. Deniau in Grenoble, France for their financial support and assistance.

References

[1] R. C. Jaeger., "Fluid transients in hydro-electric engineering practice ".Glasgow: Blackie, 1977.

[2] C. Nicolet, "Hydroacoustic modelling and numerical simulation of unsteady operation of hydroelectric systems", Thesis EPFL n° 3751, 2007, (http://library.epfl.ch/theses/?nr=3751).

[3] H. M. Paynter, "Surge and water hammer problems". Transaction of ASCE, vol. 146, p 962-1009, 1953.

[4] A. Sapin, "Logiciel modulaire pour la simulation et l'étude des systèmes d'entraînement et des réseaux électriques", Thesis EPFL n° 1346, 1995, (http://library.epfl.ch/theses/?nr=1346).

[5] O. H. Souza, Jr.; N. Barbieri; A.H.M. Santos, "Study of hydraulic transients in hydropower plants through simulation of nonlinear model of penstock and hydraulic turbine model," *IEEE Transactions on Power Systems,* vol. 14, issue 4, pp. 1269 – 1272, 1999.

[6] E. B. Wylie, & V. L. Streeter, "Fluid transients in systems". Prentice Hall, Englewood Cliffs, N.J, 1993.

[7] E. Kopf, S. Brausewetter, "Optimized control strategies for variable speed machines", *22 IAHR Symposium on Hydraulic Machinery and Systems*, Stockholm, Sweden, June 29-July 2, 2004

[8] A. Hodder, "Double-fed asynchronous motor-generator equipped with a 3-level VSI cascade", *thesis 2939*, EPFL, Lausanne, Switzerland, 2004

[9] J.-J. Simond, A. Sapin, D. Schafer, "Expected benefits of adjustable speed pumped storage in the European network", *Hydropower into the next century*, pp. 579-585, Gmunden, Austria, 1999.

[10] A. Schwery, E. Fass, J.-M. Henry, W. Bach, A. Mirzaian, "Pump storage power plants, ALSTOM's long experience and technological innovation", *Hydro 2005*, Villach, Austria, 2005